Intraplate seismicity in mid-plate South America: correlations with geophysical lithospheric parameters

HANS AGURTO-DETZEL*, MARCELO ASSUMPÇÃO, MARCELO BIANCHI &
MARLON PIRCHINER

*Institute of Astronomy, Geophysics and Atmospheric Sciences,
University of São Paulo, São Paulo 05508-090, Brazil*

Correspondence: h.agurto.detzel@gmail.com

Abstract: Mid-plate South America remains one of the least-studied regions of intraplate seismicity. Little is known about the origin and controlling factors that make this area the least seismically active intraplate region in the world. We analysed the distribution of intraplate seismicity and its correlation with several geophysical lithospheric parameters in an attempt to establish which factors might promote or inhibit the occurrence of intraplate earthquakes. We found that above-average seismicity occurs mostly in Neoproterozoic fold belts, associated with areas having a positive gravity anomaly, lower elastic thickness, higher heat flow, thinned crust and a negative S-wave anomaly at 100 km depth (associated with non-cratonic crust). Cratonic areas with a higher elastic thickness and lower heat flow are associated with low rates of seismicity. Our study suggests that the most important controlling factors are elastic thickness and heat flow. We propose that earthquake-prone areas with these favourable conditions correspond to regions of weakened lithosphere, where most of the regional lithospheric stresses are supported by the overlying brittle upper crust. These areas act as local concentrators of the regional compressional stress field, with the stress build-up then leading to the occurrence of intraplate seismicity.

Supplementary material: contains additional statistics and figures considering different filters for the used catalogue as a mean of comparison with the figures presented in the main text. They are available at http://www.geolsoc.org.uk/SUP18872

Intraplate earthquakes account for only 5% of the global release of seismic energy, but can generate vast losses in terms of human lives and resources (Talwani 2014). For example, the 1556 Shaanxi (China) earthquake (about magnitude 8) left a death toll of 830 000 victims (the deadliest earthquake on record, including plate boundary earthquakes), while, more recently, the 2001 magnitude 7.7 Bhuj (India) earthquake killed >20 000 people. Mid-plate South America, and, in particular, Brazil, is not exempt from intraplate seismicity that can cause considerable material damage and panic among a population not used to these phenomena (e.g. Chimpliganond *et al.* 2010; Agurto-Detzel *et al.* 2015). The largest registered earthquake in this area is the 1955 M_b 6.2 Porto dos Gaúchos earthquake (Barros *et al.* 2009), which is at least one unit of magnitude smaller than the maximum magnitudes registered in other intraplate regions of the world (e.g. Schulte & Mooney 2005). This fact, nonetheless, should be considered cautiously as earthquake records in South America are very recent and recurrence periods of large intraplate earthquakes are between a few hundreds and a few thousands of years (e.g. Hough 2014). Furthermore,

although intraplate earthquakes are much less frequent than plate boundary earthquakes, seismic waves are much less attenuated in stable continental lithosphere than in active areas, causing strong ground motions at large distances, which increases the hazard.

An understanding of the causes and controlling factors associated with the occurrence and distribution of intraplate events has proved to be much more elusive than an understanding of their interplate counterparts. In an early effort to explain the occurrence of intraplate seismicity on a global scale, Sykes (1978) found that these events tend to occur along pre-existing zones of weakness within areas affected by the last major orogenesis. Other researchers have explored the association of intraplate seismicity with rifted crust (e.g. Johnston & Kanter 1990; Johnston *et al.* 1994; Schulte & Mooney 2005), craton edges (e.g. Mooney *et al.* 2012), rift pillows (e.g. Zoback & Richardson 1996), areas of high heat flow (e.g. Liu & Zoback 1997), lateral density variations (e.g. Stein *et al.* 1989) and the intersection of faults (Talwani 1999).

Zoback (1992) proposed, at a lithospheric scale, the existence of a first-order mid-plate

compressional stress field (S_T), which is the product of the main plate tectonic forces, superimposed locally by a second-order stress field (S_L) associated with specific geological or tectonic features (such as lithospheric flexure, lateral strength contrasts and lateral density contrasts), which often causes a rotation of the resulting total horizontal stresses. Analyses of more recent global stress data have shown that the stress field can have several wavelengths ranging from the plate scale to the regional and local scales (Heidbach *et al.* 2010). In an attempt to combine all these findings into a unified model for intraplate earthquakes, Talwani (2014) proposed that intraplate seismicity occurs in zones where certain geological features, called local stress concentrators, promote the accumulation of local stresses, such that the interaction of this local stress field (S_L) with the regional tectonic stress field (S_T) may ultimately lead to an earthquake. The main geological features proposed as local stress concentrators lie within rifted crusts and at craton edges.

Few studies have examined the causes and distribution of intraplate seismicity for mid-plate South America. Zoback & Richardson (1996) demonstrated that local stresses associated with a rift pillow located in a failed rift in the Amazonian craton were large enough to rotate the regional stress field and produce intraplate seismicity. Assumpção (1998) noticed that, in Brazil, passive margins do not seem to be significantly more active than the average continental interior. Assumpção (1998) also found that two different patterns of seismicity arise along the Brazilian continental margin: (1) in the northeastern margin (where the continental shelf was not extended very much during Atlantic rifting), seismicity tends to occur onshore; and (2) in the southeastern margin (where the crust was highly extended during Atlantic rifting), higher seismicity occurs offshore in an area of thicker sedimentary packs. Assumpção *et al.* (2004) and Azevedo *et al.* (2015) found that higher seismicity rates occur in areas with low P-wave velocities at 150–250 km depth, interpreted as areas with a shallower asthenosphere and thus a higher geothermal gradient. In these hotter areas, the lithospheric upper mantle and lower crust have a reduced strength, thus concentrating the lithospheric stresses solely on the brittle upper crust and generating the observed seismicity. Similarly, Pérez-Gussinyé *et al.* (2007) suggested that intraplate seismicity in South America is associated with areas of lower effective elastic thickness and high heat flow and that the cold cratonic interiors would be strong enough to inhibit neotectonism. Based on gravity and stress modelling, Assumpção & Sacek (2013) proposed that flexural deformation contributes significantly to the occurrence of intraplate seismicity in mid-plate South America. Finally, Assumpção

et al. (2014) associated the occurrence of intraplate seismicity in Brazil with: (1) areas of non-cratonic crust; (2) within cratonic edges; (3) areas with flexural stresses resulting from intracrustal loads; (4) areas near neotectonic faults; and (5) areas within the passive margin.

Because intraplate events are much less frequent than interplate events, and because intraplate seismicity occurs in a wide range of geological environments, a general model explaining the occurrence of intraplate seismicity, supported by statistics and quantitative measures, has not yet been published. Moreover, a quantifiable homogeneous methodology that correlates geological or geophysical lithospheric characteristics with the occurrence of seismicity has not previously been proposed for intraplate seismicity. Our study continues previous work (e.g. Assumpção *et al.* 2004, 2014), adding new geological and geophysical variables and a more homogeneous methodology to correlate these variables with the distribution of intraplate seismicity. To that end, we want to understand where and why seismicity in mid-plate South America tends to occur more often in relation to the distribution of certain lithospheric characteristics. We hypothesize that the occurrence of intraplate seismicity in mid-plate South America is influenced by particular geological or geophysical variables that promote or inhibit local stress concentrations in certain regions, thus regulating the rates of seismicity.

Methods

Our study area is defined by the catalogue limit as shown in Figure 1. It consists of an area of 14.25×10^6 km^2 (10.95×10^6 km^2 inland and 3.30×10^6 km^2 offshore), involving the whole territory of Brazil and its passive margin and partial territories of the Guyanas, Venezuela, Bolivia, Paraguay, Argentina and Uruguay, which cover most of the inland portion of mid-plate South America.

From Figure 1, some characteristics of the distribution of seismicity can be noticed: seismicity occurs over the whole area, but it is clearly not uniform and some concentrations are observed particularly in the SE (both onshore and offshore), NE (mainly onshore, along the coast) and in a long belt roughly north–south extending from the Amazon fan through central Brazil and then Paraguay.

The catalogue

We built a declustered catalogue, filtered for M ≥ 3, giving a total of 634 events from 1767 to December 2013. The initial catalogue (1942 events) was declustered using the window method proposed by Gardner & Knopoff (1974) with the time–distance
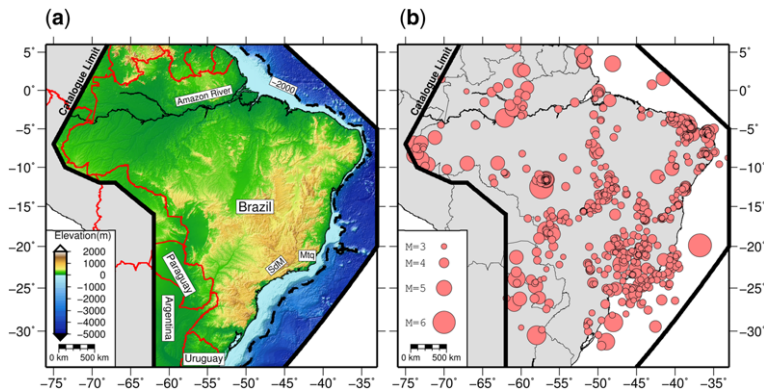
Fig. 1. (**a**) Topographic map of study area. SdM, Serra do Mar Mountain Range; and Mtq, Mantiqueira Mountain Range. The inland lines are political borders between countries. The segmented black line shows the bathymetric level −2000 m, which indicates the border of the continental shelf. (**b**) Declustered catalogue with epicentres M ≥ 3 (634 events).

windows proposed by Uhrhammer (1986). After declustering, 559 events were left out. We then filtered out events with M < 3 and depths >45 km, leaving a final catalogue with 634 events (Fig. 1). With this selection, we avoided considering recurrent sequences of foreshocks/after-shocks, deep non-intraplate events in the Peru–Brazil border and small events related to mining activities.

The catalogue is based on data from the *Brazilian Seismic Bulletin* (www.moho.iag.usp.br/portal/events#catalog), which, in turn, is based on the compilation by Berrocal *et al.* (1984), complemented since 1982 by the universities of São Paulo, Brasília and Rio Grande do Norte, and the Technological Research Institute of the state of São Paulo. Unfortunately, most events in our database do not have reliable depths and therefore we did not perform any analysis regarding the distribution in depth of the seismicity. However, previous studies indicate that intraplate seismicity in Brazil occurs at shallow crustal depths, mostly <10 km (e.g. Berrocal *et al.* 1984; Assumpção *et al.* 2014). Magnitudes vary between 3 and 6.2. The adopted magnitude scales (both equivalent to each other) are the 1-s P-wave teleseismic M_b (mostly used for events M > 4.5) and the regional magnitude M_R developed by Assumpção (1983), which uses the maximum P-wave particle velocity in the period range 0.1–1.0 s for events recorded between 200 and 2000 km. A detailed explanation on the adopted magnitude scales and magnitude completeness has been given by Assumpção *et al.* (2014).

Data processing

To analyse the distribution of seismicity in relation to the distribution of geological and geophysical variables, we used the method proposed by Hauksson (2011) applied to seismicity in California and also implemented by Agurto *et al.* (2012) to study the distribution of after-shocks of the 2010 $M_w = 8.8$ Chile earthquake. We present a set of three plots (Figs 2–10) for each geological or geophysical variable showing: (1) a map of the distributions of both the variable and the seismicity; (2) a histogram showing the normalized frequency percentage distributions of both the variable (histogram bars) and the seismicity (stepped line in histogram); and (3) a histogram showing the cumulative distribution of seismicity per bin of variable (stepped line in histogram) and the corresponding ratio R_b.

For each of the geological or geophysical variables, we first analysed its areal distribution by sampling the total area in cells of 0.1°, which correspond to the approximate average horizontal error of the events in our catalogue. We then counted the frequency of occurrence of cells for each of the considered variable ranges. For example, for the variable 'topography' (e.g. Fig. 4), we considered ranges or bins of 200 m each. For the first bin (0–200 m), we counted the frequency of occurrence of cells with topography in that range and normalized it with respect to the total number of cells. In this case, the range 0–200 m accounts for 47% of the total number of cells (i.e. 47% of the continental part of the catalogue area shown in Fig. 1). We then determined the value of the geophysical variable at each of the epicentres by bi-cubic interpolation (Wessel & Smith 1998) and calculated the normalized distribution of events occurring within each one of the parameter bins. In our example, the normalized frequency of events for the range 0–200 m is 35%. If a random distribution

of events was observed, the frequency of seismicity would match that of the areal distribution of the variable for that given range. Thus we looked for patterns of seismicity that differed from the 'expected' number of earthquakes.
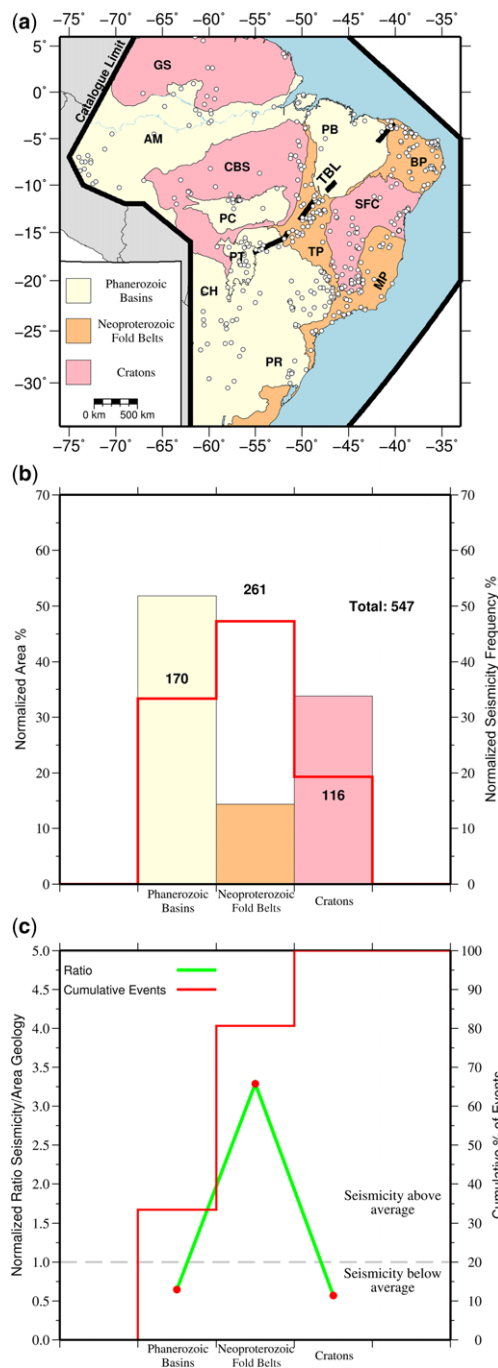
Finally, we defined and calculated for each bin a ratio $R_b = (E_B/E_B)/(V_R/V_T)$, where E_R is the number of events occurring within that bin, E_T is the total number of events, V_R is the number of cells with that parameter value within that bin and V_T is the total number of cells. Thus a value of $R_b > 1$ indicates that seismicity occurs more often than expected (above the average) and $R_b < 1$ indicates seismicity below the average. A value of $R_b \sim 1$ suggests that the seismicity occurs as often as the variable (as in a random distribution of earthquakes) and therefore no correlation exists. By using this approach, we ensured a homogeneous and quantifiable assessment of the normalized distributions of both the seismicity and the geological or geophysical variable frequencies. The use of the ratio R_b provides a quantitative measure of the occurrence of seismicity regarding the distribution of the variable.

Results

Geotectonic provinces

To investigate the possible correlations between seismicity and geotectonic setting, we divided the continental (inland) portion of our study area into three major geotectonic provinces: (1) Phanerozoic basins; (2) Neoproterozoic belts; and (3) cratonic areas (Fig. 2). These cratonic areas (e.g. the Amazon and São Francisco cratons) were stable platforms during the Brasiliano orogeny (740–580 Ma). For simplicity, we only considered those major geotectonic provinces broadly accepted in the literature (e.g. Brito Neves 2002; Assumpção *et al.* 2014). The normalized areal distribution of each province shows a dominance of Phanerozoic basins (52% of the total continental area), followed by cratonic areas (34%) and fold belt provinces, which only cover 14% of the area. Despite the low distribution of fold belts, 48% of the normalized seismicity occurs in this province, which is reflected in the ratio $R_b = 3.4$. The distribution of seismicity for the other two provinces (basins and cratons) is equally proportional to their areal distributions

Fig. 2. Distribution of seismicity versus geotectonic province. (**a**) Map showing earthquakes and tectonic features. GS, Guyana Shield; CBS, Central Brazil Shield; SFC, São Francisco Craton; AM, Amazonian Basin; PB, Parnaíba Basin; PC, Parecis Basin; PT, Pantanal Basin; CH, Chaco Basin; PR, Paraná Basin; BP, Borborema Province; TP, Tocantins Province; MP, Mantiqueira Province; and TBL, Transbrasiliano Lineament. (**b**) Histogram of frequency of seismicity and areal distribution of the geotectonic provinces. (**c**) histogram of cumulative distribution of seismicity and ratio R_b.

with a ratio $R_b \sim 0.6$. Thus the seismicity in mid-plate South America clearly correlates with the geotectonic environment in which it occurs, with seismicity occurring in Neoproterozoic fold belts 3.4 times more often than expected for a random distribution. No clear difference was observed in the seismicity rate for Phanerozoic basins and old cratonic areas, where it was around half the rate expected from a random distribution.

Non-rifted interior versus passive margin

A spatial association between intraplate earthquakes and rifted crust has been suggested by several researchers (e.g. Sykes 1978; Johnston & Kanter 1990). Schulte & Mooney (2005) found that, world-wide, 52% of intraplate earthquakes of magnitude ≥ 4.5 occur in rifted crust, with passive margins (rifted continental margins) accounting for 25%. These researchers also found that earthquakes occurring in rifted crust account for 90% of the energy released by intraplate earthquakes. This is highly significant given that the area of non-rifted crust in stable continental interiors is several times larger than the area of rifted margins. We wanted to test whether this association holds true in the case of mid-plate South America.

We separated our study area into regions of continental interior (non-rifted interior) and passive margin (rifted continental margin; Fig. 3). We defined passive margins as the area contained between the coastline and the oceanic–continental crust limit (see Assumpção *et al.* 2014 for an extended explanation). The continental interior accounts for 87% of the total area, whereas the passive margin represents the remaining 13%. Of the 632 earthquakes occurring within the total area (i.e. passive margin plus continental interior), 547 (87%) occurred within the continental interior and 85 (13%) within the passive margin area. This relationship indicates that, for mid-plate South America, there is no preference for seismicity occurring in rifted crust (continental margin) versus non-rifted crust (continental interior). If we consider the whole catalogue of events $M \geq 3$ and the unified catalogue, a similar relation is found.

Topography

We only considered the continental area for the topographic analysis as the low frequency and wide range of offshore topography bins might have masked the real distributions inland. In any case, the observed characteristics are similar if we consider the whole area (inland + offshore). For this analysis, we used the global topography grid ETOPO1 (Amante & Eakins 2009) with a resolution of 1 arc-minute. The lowest and highest
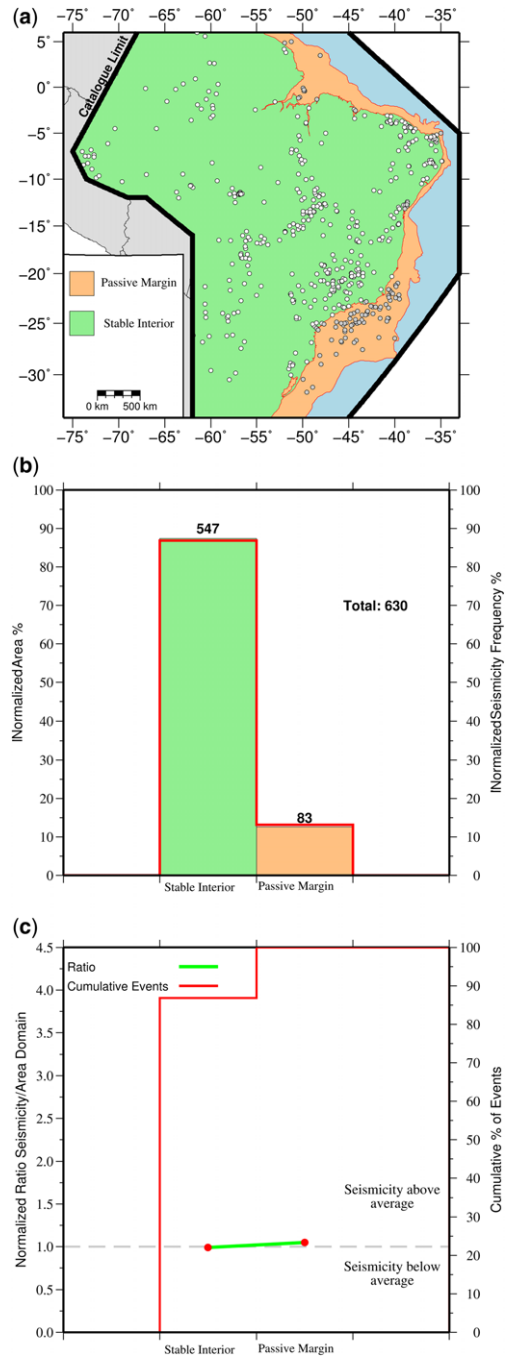

Fig. 3. Distribution of seismicity versus rifted/non-rifted crust. (**a**) Map showing earthquakes over areas of non-rifted crust (continental interior) and rifted crust (passive margin). (**b**) Histogram of frequency of seismicity and areal distribution of rifted/non-rifted crust. (**c**) Histogram of cumulative distribution of seismicity and ratio R_b.

topographic values are -100 and 2385 m, respectively, with an average altitude of 297 m for the inland area considered. Higher topography is observed in the eastern part of Brazil, along the Mantiqueira and Serra do Mar mountain ranges (Figs 1a & 4a), whereas the lowest values are found in the coastline and around the Amazonian basin. The frequency distribution of the topographic values constantly decays towards higher values, with almost 50% of the nodes presenting values <200 m (Fig. 4b). The seismicity distribution tends to follow the topography distribution, indicating that this variable would not critically affect the occurrence of seismicity. Nevertheless, higher ratios of up to $R_b = 2.2$ are observed for the bins between 600 and 1400 m. The lowest seismicity rate is observed for the range 0–200 m, with 35% of the earthquakes and a ratio $R_b = 0.75$. The lower than expected occurrence of seismicity in the range 0–200 m is highly significant with a probability $p(\text{quakes} \leq 35\%) = 1.9 \times 10^{-8}$, whereas the higher rates of seismicity observed in the range 600–1200 m are also statistically significant with $p(\text{quakes} \geq X\%) < 0.05$. In conclusion, a higher than average seismicity rate (about two times) is observed for higher values of topography between 600 and 1200 m and lower seismicity than expected is observed for the lower range 0–200 m. For the range 200–600 m, the seismicity rate is not significantly different from that expected and therefore the topography might not control decisively the occurrence of earthquakes in this topographic range.

Gravity anomaly

Residual gravity anomalies reflect the distribution of lateral density variations within the crust. We used the satellite-derived European Space Agency's Gravity Field and Steady-state Circulation Explorer free air gravity anomaly model to test whether variations in crustal density have an impact on the distribution of intraplate seismicity in mid-plate South America (Fig. 5). The histogram of gravity anomalies shows a normal distribution with extreme values of -74 and 79 mGal and an average value of -2 mGal. Negative anomalies are found mainly offshore (just off the continental shelf) and in the Paraná and Parnaíba basins. Positive anomalies are found in the west, closer to the Andes and along the Transbrasiliano Lineament (TBL). Most of the seismicity is concentrated in areas of positive gravity anomaly: 57% of the total events occur within positive anomalies and the remaining 43% in areas with negative gravity anomalies. Furthermore, 79% of the seismicity occurs in areas with a gravity anomaly greater than -10 mGal, although this gravity range involves only 61% of the total area. Accordingly,
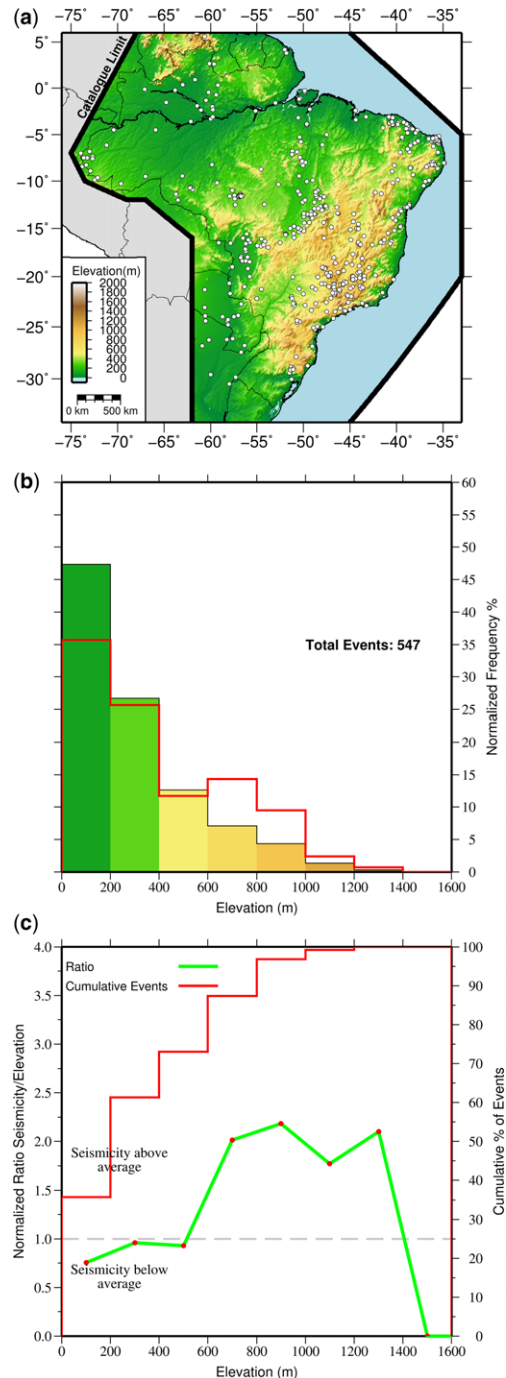

Fig. 4. Distribution of seismicity versus topography. (**a**) Map showing earthquakes over topography grid. (**b**) Histogram of frequency of seismicity (stepped line) and areal distribution of each bin of topography values (bars). (**c**) Histogram of cumulative distribution of seismicity (stepped line) and ratio R_b.
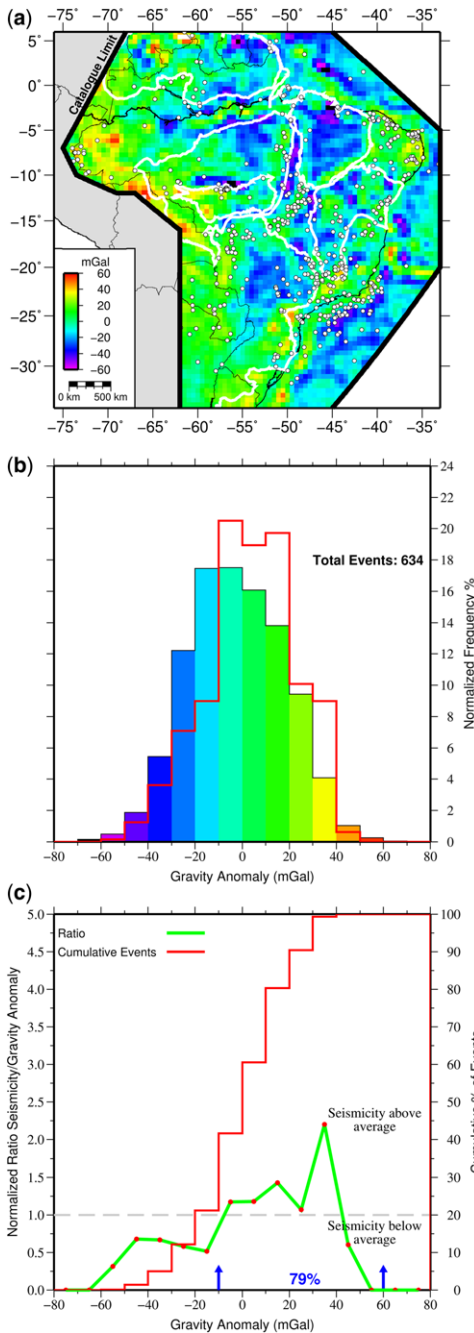
Fig. 5. Distribution of seismicity versus gravity anomaly. (**a**) Map showing earthquakes over gravity anomaly grid. The geotectonic provinces of Figure 2 are delineated in white. (**b**) Histogram of frequency of seismicity (stepped line) and areal distribution of each bin of gravity anomaly values (bars). (**c**) Histogram of cumulative distribution of seismicity (stepped line) and ratio R_b.

ratios of $R_b < 1$ are observed for areas with a gravity anomaly less than -10 mGal, whereas $R_b > 1$ ratios are found in areas with anomalies between -10 and 40 mGal (Fig. 5c). In conclusion, it seems that higher than average seismicity mostly occurs in areas of average (close to 0) and positive (greater than -10 mGal) anomalies, some of them related to the regions of Neoproterozoic fold belts described in this paper, such as the TBL and Tocantins province. On the other hand, areas with high negative gravity anomalies, such as the Paraná and Parnaíba basins and the Guyana craton, tend to have below average seismicity.

Elastic thickness

The flexural rigidity or effective elastic thickness, T_e, is commonly used to characterize the state of mechanical strength of the lithosphere. Pérez-Gussinyé *et al.* (2007) found that intraplate seismicity in South America tends to occur more often in areas with lower values of T_e, implying that cratonic interiors (with higher values of T_e) are strong enough to inhibit tectonism, and that intraplate deformation tends to occur within thin, hot and hence weak lithosphere. Here we revisit these findings, expanding the earthquake catalogue and using a new T_e database. The new T_e grid (Pérez-Gussinyé, pers. comm. 2014) was built by combining windows of 400×400, 600×600 and 800×800 km^2 (Pérez-Gussinyé *et al.* 2009a, b) to obtain a unified grid with a resolution of $0.5°$.

The map of T_e (Fig. 6a) shows that 42% of the total area corresponds to cells with $T_e > 100$ km, mainly located in the interior of the continent. Low values of T_e are found along the continental edge and in the oceanic crust. Noteworthy is the presence of intermediate T_e values ($30-70$ km) near the Tocantins Province (and beneath the Paraná Basin) in the centre of our study area. The distribution of seismicity tends to follow that of the T_e, i.e. the ratios R_b are close to one for the different T_e bins, except for $T_e < 30$ km and $T_e > 100$ km (Fig. 6b, c). It appears that above-average seismicity occurs in areas with low T_e (<30 km), such as near the coast in northern Brazil and in the southeastern offshore area. The highest ratio ($R_b \sim 3.9$) is found for the T_e range $0-10$ km and is mostly due to the high seismicity occurring in one particular area of the Borborema Province (NE tip of Brazil). The lowest ratio ($R_b = 0.65$) is found for very large values of T_e ($T_e > 100$ km), such as in the Amazonian craton), indicating that zones with a thicker T_e tend to have lower seismicity rates. For this bin ($T_e > 100$), the expected number of earthquakes for a random distribution would be 266 (42% of the total 634 quakes), but instead we only observed 174 (27.4%), which is highly significant with a

probability p (quakes ≤ 174) $= 1.9 \times 10^{-14}$. Similarly, for the bins $T_e < 30$ km the difference between the expected and observed number of earthquakes is statistically significant ($p < 0.05$). In

(a)

(b) Total Events: 634

(c)
Ratio
Cumulative Events

Normalized Ratio Seismicity/Elastic Thickness

Seismicity above average

Seismicity below average

Elastic Thickness (km)

summary, it appears that effective elastic thickness is an important variable in determining the occurrence of intraplate seismicity. Areas with lower elastic thickness, $T_e < 30$ km, tend to have higher seismicity rates ($R_b \sim 1.4$), whereas areas with high T_e values ($T_e > 100$ km) present lower seismicity rates ($R_b = 0.65$).

Heat flow

Heat flow measurements reflect the thermal state of the lithosphere. For example, old cratonic areas present low heat flow, whereas newer oceanic crust presents higher than average heat flow. Liu & Zoback (1997) proposed that intraplate seismicity is associated with areas of elevated temperature at depth, in which plate-driving forces are largely supported by the upper crust because the lower crust and upper mantle are relatively weak. We wanted to test whether seismicity in mid-plate South America shows any correlation with heat flow data. We hypothesized that lower than average seismicity occurs in cold cratonic areas, whereas seismicity tends to concentrate in areas of higher heat flow. We used the world heat flow database published by Davies (2013), which contains heat flow cells of $2 \times 2°$. The heat flow data for South America used by Davies (2013) is largely based on the compilation by Hamza *et al.* (2005), which, unfortunately, has a very sparse distribution in Brazil. Figure 7 shows the distribution of heat flow values and seismicity in our study area. In general, mid-plate South America presents low temperatures, with an average of 60 mW m^{-2} in the continental area. Despite the low resolution of the grid, it is possible to individualize areas of low heat flow, such as the Amazon craton in the north, and others of higher heat flow, such as in the continental margin. Around 97% of the area presents heat flow values <80 mW m^{-2}, with $>75\%$ of the area showing values between 50 and 70 mW m^{-2}. Despite this prevalence of values <80 mW m^{-2} (97% of the area), the distribution of seismicity shows the occurrence of only 76% of seismicity in cells with heat flow values in this range. In particular, the heat flow bin 60–70 mW m^{-2}, which occupies almost 50% of the study area, contains only 40% of the normalized seismicity. Accordingly, the
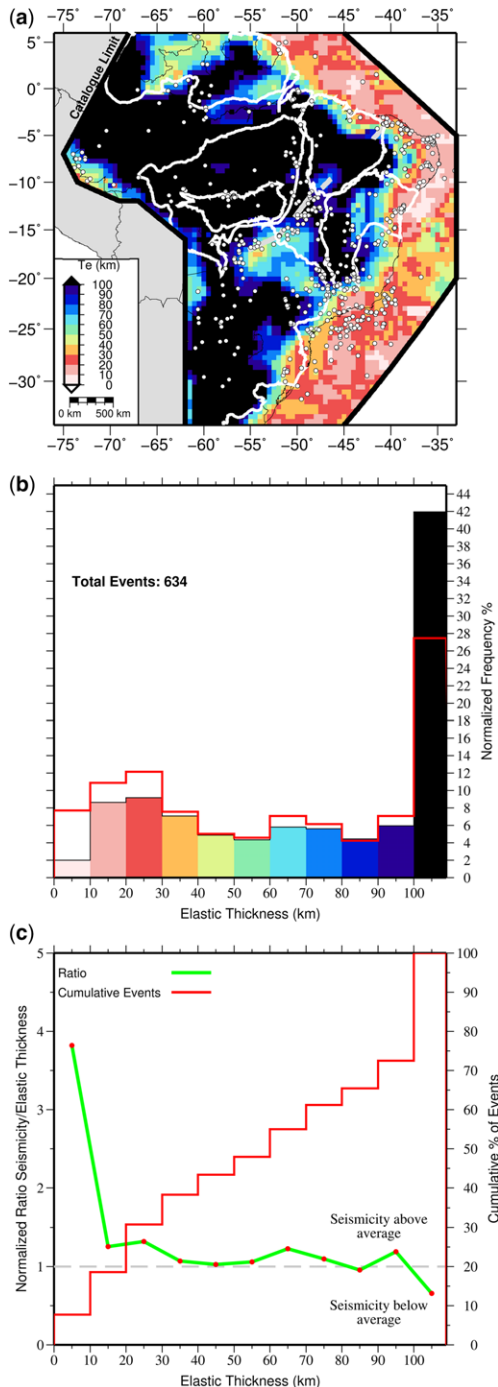
Fig. 6. Distribution of seismicity versus effective elastic thickness. (**a**) Map showing earthquakes over elastic thickness grid. The geotectonic provinces of Figure 2 are delineated in white. (**b**) Histogram of frequency of seismicity (stepped line) and areal distribution of each bin of elastic thickness values (bars). (**c**) Histogram of cumulative distribution of seismicity (stepped line) and ratio R_b.
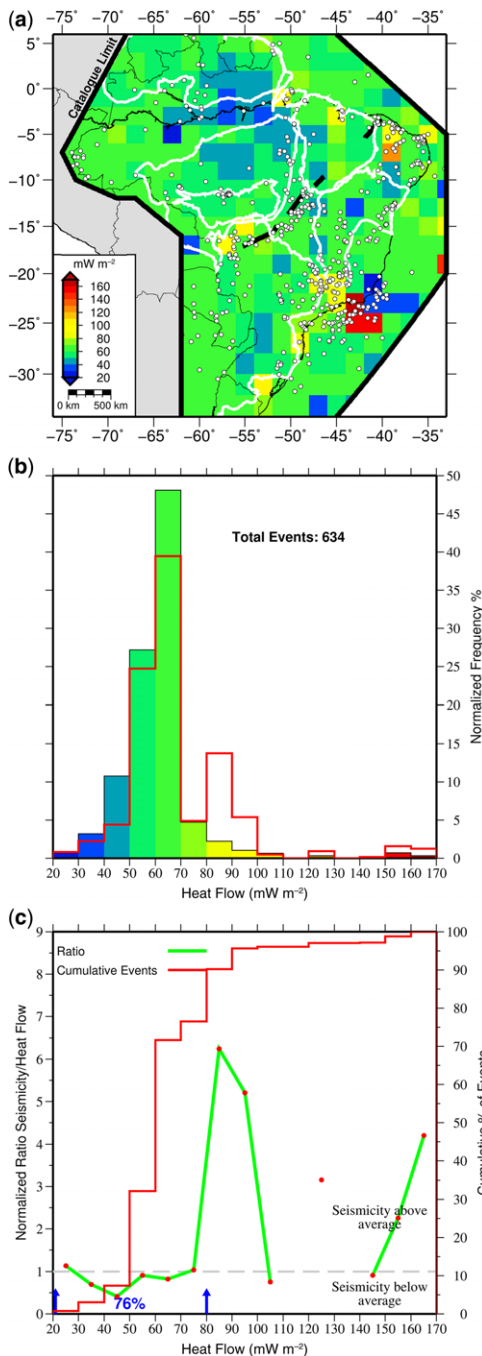
Fig. 7. Distribution of seismicity versus heat flow.
(**a**) Map showing earthquakes over heat flow grid. The geotectonic provinces of Figure 2 are delineated in white. (**b**) Histogram of frequency of seismicity (stepped line) and areal distribution of each bin of heat flow values (bars). (**c**) Histogram of cumulative distribution of seismicity (stepped line) and ratio R_b.

ratio of seismicity to heat flow is much higher than 1.0 (seismicity well above average) for the range 80–100 mW m^{-2} and particularly low (seismicity below average) for the heat flow bin 40–50 mW m^{-2}. In conclusion, seismicity tends to occur at above-average frequencies in areas with heat flow >80 mW m^{-2} and less frequently in areas of low heat flow, such as cold cratonic areas.

Crustal thickness

Using Moho depth constraints, we wanted to test whether the occurrence of seismicity shows any correlation with crustal thickness. The grid of crustal thickness used was Model A of Assumpção *et al.* (2013*a*) based on receiver functions and seismic refraction lines (Fig. 8). The deeper Moho depths are found within the Guyana and Central Brazil shields, the São Francisco craton and to the SW of this craton in the Paraná Basin. Moho depths shallower than 35 km are found in the central part of the study area around the TBL and near the continental border, whereas the shallowest values occur within the oceanic crust. The extreme crustal thickness values found within our study area are 10 and 50 km, with a mean of 34 km (extreme values of 24 and 50 km with a mean of 38.5 km for the inland portion). Most of the area (67%) presents a crustal thickness between 35 and 45 km, but this range contains only 59% of the seismicity. For this range (35–45 km), the observed seismicity is significantly lower than that expected for a random distribution of earthquakes. On the other hand, seismicity rates well above average are found for the crustal thickness range 25–35 km, which corresponds to thinned continental crust near the margin and stretched continental crust beneath the continental shelf. The lowest rates are observed for areas with a Moho depth shallower than 20 km (i.e. mainly oceanic areas); areas with Moho depths between 35 and 45 km also present slightly lower than average seismicity rates ($R_b \sim 0.9$). In conclusion, inland seismicity tends to occur more frequently than expected in areas of thinned continental crust with Moho depths shallower than 35 km. A lower seismicity rate is observed in areas with deeper Moho (thicker crust), in particular for the range 35–45 km, which covers most of the inland area.

Lithospheric S-wave velocity anomaly (cratonic versus non-cratonic lithosphere)

Using the shear-wave velocity perturbation (δV_S) at a depth of 175 km, Mooney *et al.* (2012) defined areas of cratonic and non-cratonic lithosphere worldwide and found that intraplate seismicity with magnitudes >4.5 tends to concentrate at
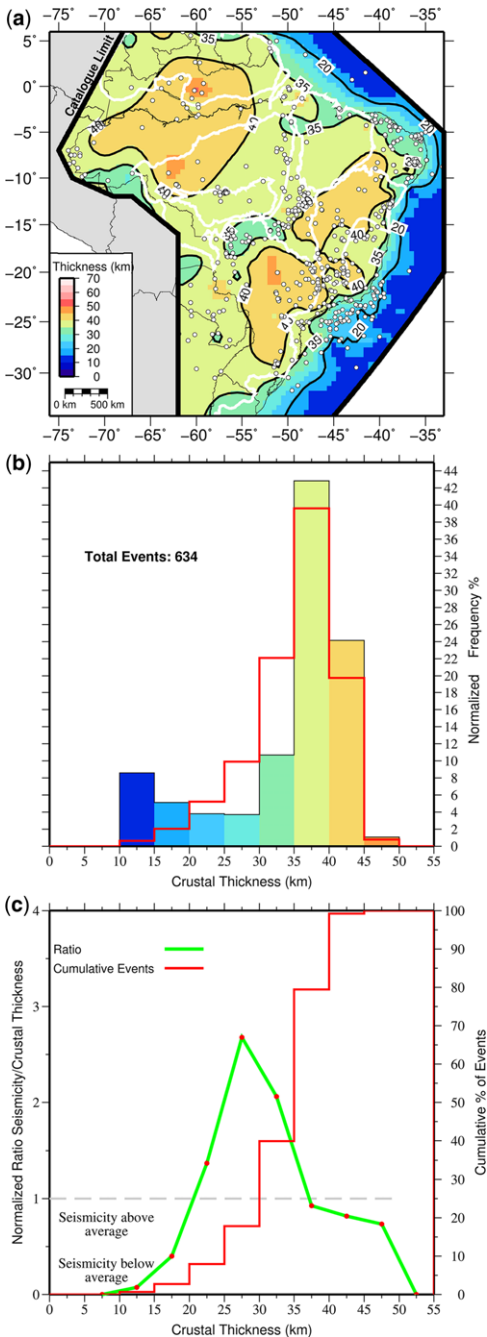
Fig. 8. Distribution of seismicity versus crustal thickness. (**a**) Map showing earthquakes over crustal thickness grid. The geotectonic provinces of Figure 2 are delineated in white. (**b**) Histogram of frequency of seismicity (stepped line) and areal distribution of each bin of crustal thickness values (bars). (**c**) Histogram of cumulative distribution of seismicity (stepped line) and ratio R_b.

cratonic edges and that cold, stable cratonic interiors ($\delta V_S > 3.5\%$) have significantly fewer earthquakes. To test this hypothesis for mid-plate South America, we analysed the distribution of seismicity versus the S-wave anomaly data obtained from a joint inversion of surface waves and receiver functions (Assumpção *et al.* 2013*a*; Fig. 9). The S-wave velocity anomalies were measured with respect to a reference model (in this case, IASP91) and are interpreted in terms of cratonic and non-cratonic lithosphere. For our study area, the δV_S values range from -7 to 7% with an average of 1% δV_S anomaly. Zones of high S-wave anomaly ($\delta V_S > 5\%$) are found in the cratonic areas such as the Guyana and Central Brazil shields, with another high S-wave anomaly to the south and SW of the São Francisco craton. Negative S-wave anomalies are found in the oceanic area, near the continental margin and beneath the Chaco Basin (northern Argentina and Paraguay) and the Pantanal Basin in central-west Brazil. The distribution of seismicity shows, in general, a higher frequency of events in regions with negative anomalies (δV_S less than -1%), accounting for 44% of the total seismicity and a higher than average seismicity in areas with δV_S between 3 and 5%, accounting for 26% of the seismicity. The maximum ratio R_b (seismicity/S-wave anomaly) is found for the δV_S range -6 to -5% ($R_b = 3.5$), although this has to be considered with caution given that regions within this δV_S range only account 1% of the total area. On the other hand, regions with average S-wave velocity anomalies (-1 to 3%) present the lowest seismicity rates, with the ratio $R_b \sim 0.55$, and account for only 26% of the total seismicity despite covering 45% of the total area. Regions with anomalies $\delta V_S > 5\%$ also present low levels of seismicity ($R_b \sim 0.7$). In summary, areas with average δV_S (-1 to 3%) and high $\delta V_S > 5\%$ tend to have low rates of seismicity, whereas areas with negative anomalies δV_S less than -1% show higher than average levels of seismicity. The occurrence of higher than average seismicity in the δV_S range $3-5\%$ probably reflects the cratonic edge effect found by Mooney *et al.* (2012) and confirms the initial findings of Assumpção *et al.* (2014).

Crustal average V_p/V_s ratio

We created a new map of average crustal V_p/V_s ratios for the continental part of our study area based on the integration of several published datasets (e.g. Bianchi 2008; Assumpção *et al.* 2013*b* and references cited therein; Fig. 10). Each reported value was averaged when corresponding to a repeated station and the final map was produced by interpolation of the median values gridded every $2 \times 2°$. Extreme values (<1.68, >1.82)

were removed before computation of the grid, as well as points with a discrepancy >0.5. We observe V_p/V_s values between 1.69 and 1.82, with a mean of 1.73 for the total area. Low V_p/V_s values are observed in the interior of the continent, mostly in cratonic areas, whereas the higher values are closer to the coast. The seismicity mostly concentrates at average values between 1.71 and 1.75 (71% of the seismicity). For this range, higher than average seismicity is observed with ratios R_b between 1.0 and 1.5. The seismicity rate decreases towards the extremes, following the distribution of the variable. Thus V_p/V_s ratios do not seem to exert a major influence on the occurrence of seismicity, with 56% of the seismicity occurring for values below the general average (1.69–1.73) and 44% occurring in the upper range (1.73–1.83).

Discussion

The following analyses were performed only for the continental region (see Fig. 2) as this area presents more accuracy on the sampled parameters and can be divided into the three geotectonic provinces considered. Also, including offshore data for analysis of the correlation between variables artificially increases the degree of correlation between variables given that most of the crustal parameters exhibit first-order differences between onshore and offshore values.

Geotectonic provinces

As expected, a clear dependency exists between seismicity and the geotectonic environment. A variance analysis of the average number of earthquakes per sampled node (0.5°) shows that the seismicity in fold belts is significantly different (higher) than the seismicity in the other two areas ($p < 0.05$). Thus Neoproterozoic fold belts present higher tectonic activity – in this case, 3.4 times higher than expected for a random distribution of earthquakes (see Fig. 2). On the other hand, the Phanerozoic basins and cratonic areas present similar lower rates of seismicity, around half that expected for their respective areas.

Once it had been established that fold belts present significantly more seismicity than the other two geotectonic provinces, we wanted to explore which geophysical parameters characterized each province and whether these parameters could explain the observed distribution of seismicity. Table 1 gives
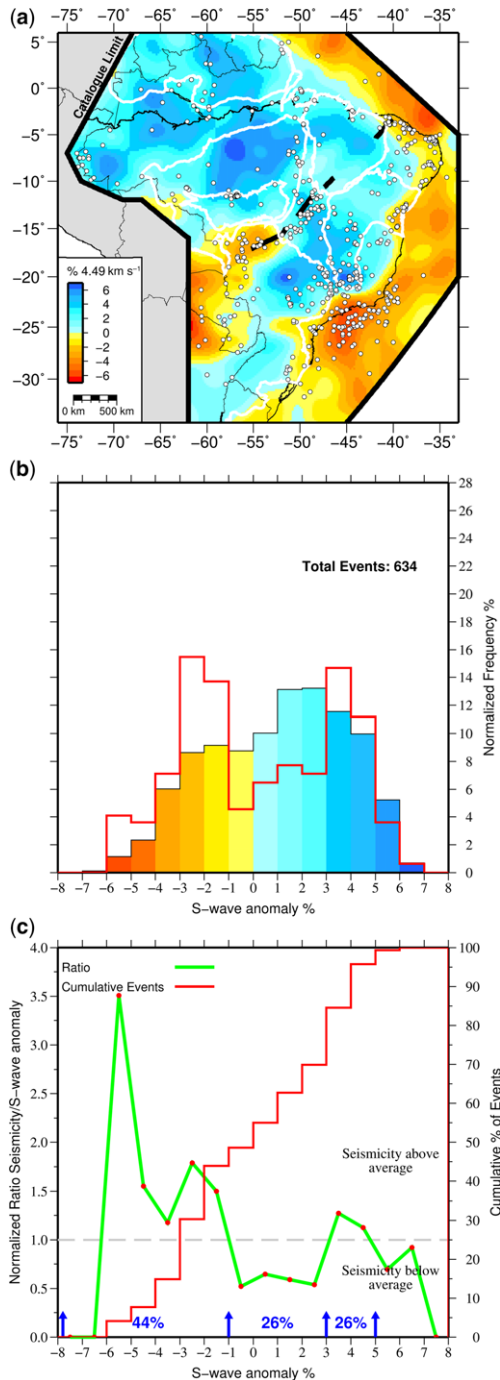

Fig. 9. Distribution of seismicity versus S-wave anomaly at 100 km depth. (**a**) Map showing earthquakes over S-wave anomaly grid. The geotectonic provinces of Figure 2 are delineated in white. (**b**) Histogram of frequency of seismicity (stepped line) and areal distribution of each bin of S-wave anomaly values (bars). (**c**) Histogram of cumulative distribution of seismicity (stepped line) and ratio R_b.
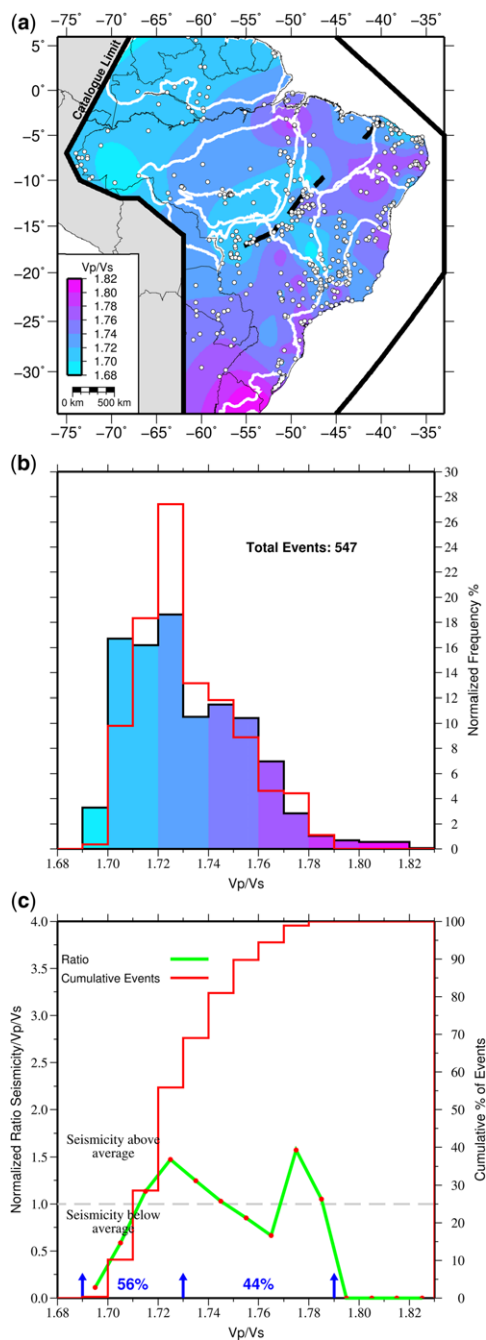
Fig. 10. Distribution of seismicity versus crustal average V_p/V_s ratios. (**a**) Map showing earthquakes over V_p/V_s grid. The geotectonic provinces of Figure 2 are delineated in white. (**b**) Histogram of frequency of seismicity (stepped line) and areal distribution of each bin of V_p/V_s values (bars). (**c**) Histogram of cumulative distribution of seismicity (stepped line) and ratio R_b.

the descriptive statistics for each geophysical variable for the three geotectonic provinces. In comparison with the Phanerozoic basins and cratonic areas, the Neoproterozoic fold belts are distinctively characterized by: (1) higher values of topography, heat flow and V_p/V_s ratios; (2) lower values of elastic thickness, crustal thickness and S-wave anomaly; and (3) lower (closer to 0) free air gravity anomalies.

Another way of visualizing these differences is shown in Figure 11, which presents the value of each considered geophysical parameter at the position of each one of the 547 inland earthquakes. Each line therefore represents an earthquake coloured according to the geotectonic province in which it occurs. It seems that earthquakes that occur in fold belts (green lines) tend to concentrate at lower values of T_e and crustal thickness and at higher values of heat flow. Earthquakes in cratonic areas (blue lines) concentrate, for example, at high values of S-wave anomalies and present the highest crustal thickness values. The most dispersed parameters appear to be topography and gravity anomaly, for which earthquakes of the three geotectonic provinces seem to occur at all values. Thus the higher rates of seismicity observed in fold belts could be explained by the crustal parameters that characterize this geotectonic province. In this sense, earthquakes would preferentially occur in areas with higher topography, heat flow and V_p/V_s ratios, and in areas with a lower elastic thickness, crustal thickness and S-wave anomaly.

Correlations between crustal parameters and earthquake occurrence

To better understand the relationships between each of the geophysical parameters and the occurrence of seismicity, we calculated their respective correlation coefficients. We sampled our study area in cells of 0.5° and calculated the values of each geophysical parameter, including the number of earthquakes, in each cell. The results are shown in Table 2. Larger correlations are observed for crustal thickness with S-wave anomaly (0.48) and with elastic thickness (0.32); and for S-wave anomaly with heat flow (−0.38), with elastic thickness (0.36) and with gravity anomaly (−0.33). The relations among these variables can be explained as follows: a thicker crust, such as in cratonic areas, presents a high S-wave anomaly (cratonic roots), a higher effective elastic thickness and a low heat flow (older, thus colder lithosphere). Another interesting correlation is observed between S-wave anomalies and V_p/V_s ratios (−0.28), which can be interpreted in terms of Archean cratonic areas (which present high positive S-wave anomalies)

Table 1. *Median, mean and standard deviation (SD) values of the sampled geophysical parameters for each geotectonic province*

	Basins			Fold belts			Cratons		
	Median	Mean	SD	Median	Mean	SD	Median	Mean	SD
Topography (m)	155	237	215	369	444	321	241	324	254
Gravity anomaly (mGal)	3.46	2.02	20.43	2.60	0.60	20.18	−3.94	−2.82	20.91
Elastic thickness (T_e) (km)*	101.0	90.4	18.3	62.6	63.1	30.9	101.0	86.2	22.5
Heat flow (mW m^{-2})	61.4	60.4	10.4	61.8	67.0	21.0	58.1	56.1	8.2
Crustal thickness (km)	38.1	38.4	3.0	37.5	36.8	3.6	39.2	39.3	2.7
S-wave (%)	1.92	1.70	2.33	0.68	0.73	2.33	2.89	2.92	1.87
V_p/V_s	1.732	1.733	0.024	1.742	1.744	0.026	1.722	1.723	0.018

*Elastic thickness with values >100 km were fixed to 101 km.

being composed of a more felsic crust that lacks a mafic underplated lower crust (i.e. without a high-velocity mafic basal layer; e.g. Durrheim & Mooney 1994) and therefore presenting lower V_p/V_s ratios (see Fig. 10).

Regarding those variables that correlate better with earthquake occurrence, we observed that the maximum correlation occurs with T_e (−0.14), indicating, once again, that higher seismicity occurs in areas with a lower elastic thickness. For the rest of the variables, we see that seismicity is associated with higher heat flow (0.10), thinner crust (−0.09) and S-wave anomalies (−0.07). On a second order of correlation, we see that earthquake occurrence

is related to higher topography (0.05) and gravity values (0.05), whereas V_p/V_s ratios seem to have a much weaker relation (0.01).

To explore the ranges of values of each geophysical parameter at which most earthquakes occur, we calculated the mean, median and standard deviation of the geophysical variables at each inland earthquake and for the inland area in general (Table 3). We observed that there are clear differences between the average values of each parameter measured for earthquakes and for the area. For example, inland earthquakes tend to occur in regions with higher topography and a higher positive gravity anomaly than the average height
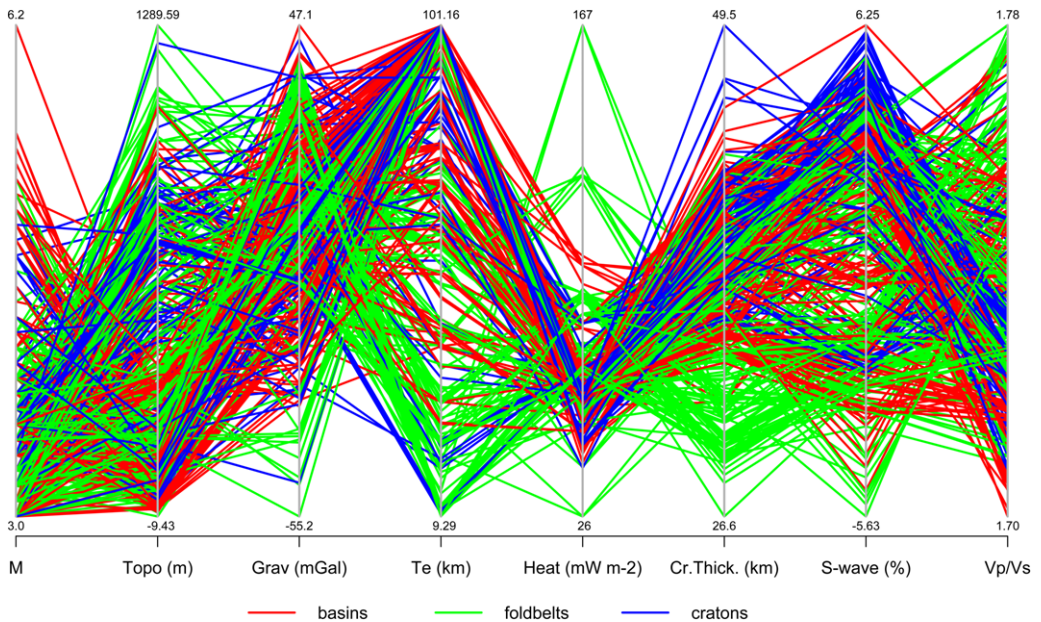

Fig. 11. Sampled geophysical parameters for inland earthquakes. Each earthquake is represented by a line coloured according to its geotectonic province. See text for further explanation.

Table 2. *Correlation coefficients for number of quakes and sampled variables in inland areas*

	No. of earthquakes	Topography	Gravity anomaly	T_e	Heat flow	Crustal thickness	S-wave	V_p/V_s
No. of earthquakes	1.00	0.05	0.05	−0.14	0.10	−0.09	−0.07	0.01
Topography	0.05	1.00	0.01	−0.17	0.02	0.21	0.01	0.07
Gravity anomaly	0.05	0.01	1.00	−0.06	0.20	−0.19	**− 0.33**	−0.09
T_e	−0.14	−0.17	−0.06	1.00	−0.18	**0.32**	**0.36**	−0.09
Heat flow	0.10	0.02	0.20	−0.18	1.00	−0.31	**− 0.38**	0.09
Crustal thickness	−0.09	0.21	−0.19	**0.32**	−0.31	1.00	**0.48**	−0.12
S-wave	−0.07	0.01	**− 0.33**	**0.36**	**− 0.38**	**0.48**	1.00	**− 0.28**
V_p/V_s	0.01	0.07	−0.09	−0.09	0.09	−0.12	**− 0.28**	1.00

Values in **bold** indicate higher correlations (see text).

and gravity anomaly of the inland area, respectively. Further, earthquakes tend to occur more often where the elastic thickness is lower, the heat flow is higher and the crustal thickness is thinner than their respective averages for the inland area. Lastly, the mean and median values of the *S*-wave anomaly measured for earthquakes indicate that earthquakes tend to occur in regions with lower S-wave anomaly, whereas no noticeable difference is observed in terms of preference for certain values of V_p/V_s ratios.

The higher rates of seismicity in Neproterozoic fold belts are statistically significant and can be explained as the lithosphere of stable cratonic areas tending to be strong enough to inhibit neotectonic activity, whereas fold belts are more likely to have zones of weakness where earthquakes occur in inherited structures. Accordingly, a set of geophysical parameters that characterize these areas of higher seismicity also delineates the most crucial parameters in terms of influence on the occurrence of earthquakes. In mid-plate South America, and relative to the average geophysical values of the sampled area, earthquakes tend to occur in areas with higher topography, positive gravity anomalies, lower elastic thickness, higher

heat flow values, thinner crust and negative S-wave anomaly values.

Although higher than average levels of seismicity seem to occur in areas with higher topography (>600 m), the low correlation coefficient between earthquake occurrence and topography (0.05) discards this variable as an important controlling factor. Recent thermochronological studies have indicated that there is a relationship between topography and neotectonics in SE Brazil (e.g. Cogné *et al.* 2012). However, the relationship between topography and tectonic activity is poorly known in mid-plate South America and further studies are needed to address this issue.

The higher than average seismicity found for positive gravity anomalies can be explained as a consequence of the superposition of regional stresses with local flexural stresses, as suggested by Assumpção & Sacek (2013) for central Brazil. Similarly, the occurrence of higher rates of seismicity in areas with lower elastic thickness and higher heat flow indicate an analogous process of local stress concentration. These areas correspond to regions with a hot and weak upper mantle lid (thinned lithosphere), where the lithospheric stresses are supported mainly by the strong, brittle

Table 3. *Median, mean and standard deviation (SD) values for each geophysical parameter for inland earthquakes (Q) and inland study area (A)*

	Inland earthquakes (547)			Inland study area		
	Median Q	Mean Q	SD Q	Median A	Mean A	SD A
Topography (m)	312	387	304	213	297	257
Gravity anomaly (mGal)	7.6	6.23	18.23	0.87	0.23	20.49
T_e (km)*	71.8	65.3	35.0	101.0	85.0	23.9
Heat flow (mW m^{-2})	62.7	67.7	15.6	60.6	60.0	12.1
Crustal thickness (km)	37.6	36.9	4.1	38.5	38.5	3.1
S-wave (%)	1.11	0.92	2.88	2.17	1.96	2.32
V_p/V_s	1.728	1.733	0.019	1.726	1.732	0.024

*Elastic thickness with values over 100 km were fixed to 101 km.

upper crust. Thus a local disturbance and concentration of the regional compressional stress field occurs, eventually leading to an earthquake. To summarize, stress concentration in the upper crust can be due to: (1) a weak and thinned lithosphere (shallow asthenosphere) characterized by low elastic thickness, high heat flow values and low S-wave anomalies; and/or (2) flexural stresses caused by crustal loads in areas of thin crust (high positive free air gravity anomalies) and low elastic thickness. On the other hand, a thicker, cold and therefore stronger crust, such as in cratonic areas, presents significantly lower levels of seismicity. This is particularly reflected by the lower than average levels of seismicity observed in areas with high elastic thickness ($T_e > 100$ km), low heat flow (<70 mW m^{-2}) and high S-wave anomaly ($>5\%$).

Consequently, we have found that there are certain geophysical variables that seem to exert a major influence on the occurrence of seismicity, whereas others have a lesser or no impact. The variables that appear not to have any impact are rifted versus non-rifted crust and V_p/V_s ratios. All the other variables show certain ranges of values that seem to promote (or inhibit) the occurrence of earthquakes. In this sense, the geotectonic province is the variable that shows the most evident correlation with seismicity.

Some earlier studies (e.g. Johnston & Kanter 1990; Johnston *et al.* 1994; Schulte & Mooney 2005; Assumpção *et al.* 2014) have suggested that there is a preference for intraplate earthquakes to occur in regions of rifted crust – in particular, passive margins –compared with non-rifted regions. We observed that this does not hold true for Brazil, where we found the same number of expected events for rifted (continental shelf) and non-rifted crustal regions according to their respective areas (Fig. 3). Assumpção (1998) made a similar observation by comparing qualitatively the seismicity in the Brazilian interior and passive margin. Schulte & Mooney (2005) suggested that, on a global scale, the correlation between intraplate earthquakes and rifted crust has been overestimated in the past. Figure 3 shows that seismicity is not uniform along the Brazilian passive margin, indicating that other factors (such as high stretching ratios in the pre-rift process and flexural effects from a thick sedimentary load) should be more important than just the rifted nature of the crust.

Conceptual model

Figure 12 shows the correlations found in this work, presenting a lithospheric cross-section based on actual data. In this section, the Borborema Province (BP) shows the highest levels of seismicity, with clusters occurring in the NE tip of the province and to the northern edge of it. The lithosphere here is the thinnest in the continental area considered and, in general, this geotectonic province presents a lower elastic thickness and higher heat flow than the surrounding areas (Figs 6 & 7), prompting the generation of seismicity. On the other hand, for the Parnaíba Basin and Central Brazilian Shield, the levels of seismicity are much lower. These areas are characterized by a thicker lithosphere, with a low heat flow and greater elastic thickness, characteristics that seem to inhibit the occurrence of seismicity. Some other events occur in the Tocantins Province, which also presents a thinner lithosphere and high positive gravity anomalies. A few earthquakes also occur in the border between the Tocantins Province and the Central Brazilian Shield, probably associated with the described craton-edge effect. We propose that, in intraplate regions, seismicity occurs in areas where regional stresses, derived from the plate-driving forces, concentrate locally as a result of the conjunction of particular geophysical characteristics. Among these characteristics, we propose thinned lithosphere and high heat flow to be the main controlling factors, which, in turn, will produce low values of the elastic thickness. Other factors also play an important role locally, such as density contrasts (causing flexural stresses) and cratonic edges.

Our study highlights the importance of heat flow and elastic thickness as determinant controlling factors in the occurrence of seismicity in mid-plate South America, as indicated by their correlation coefficients. Similar to the model proposed by Liu & Zoback (1997), our study suggests that, within intraplate regions, areas with a weak lithosphere characterized by high heat flow or lower elastic thickness are prone to accumulate elastic deformation in the upper crust, ultimately leading to the generation of intraplate earthquakes. This occurs because in areas with high heat flow and/or lower elastic thickness, the regional compressional stresses resulting from plate-driving forces are mostly supported by the upper crust, whereas the rest of the lithospheric section (lower crust and upper mantle with relatively high temperatures) is rather weak and thus unable to support elastic stresses. In contrast, in areas with higher elastic thickness and/or low heat flow, such as cold cratonic areas, the cumulative strength of a thicker lithosphere surpasses the regional stresses of plate-driving forces, which are now absorbed not only by the upper crust, but also by the lower crust and upper mantle, preventing the generation of intraplate seismicity.

We have implemented a homogeneous and quantifiable methodology to establish the correlations between lithospheric characteristics and the
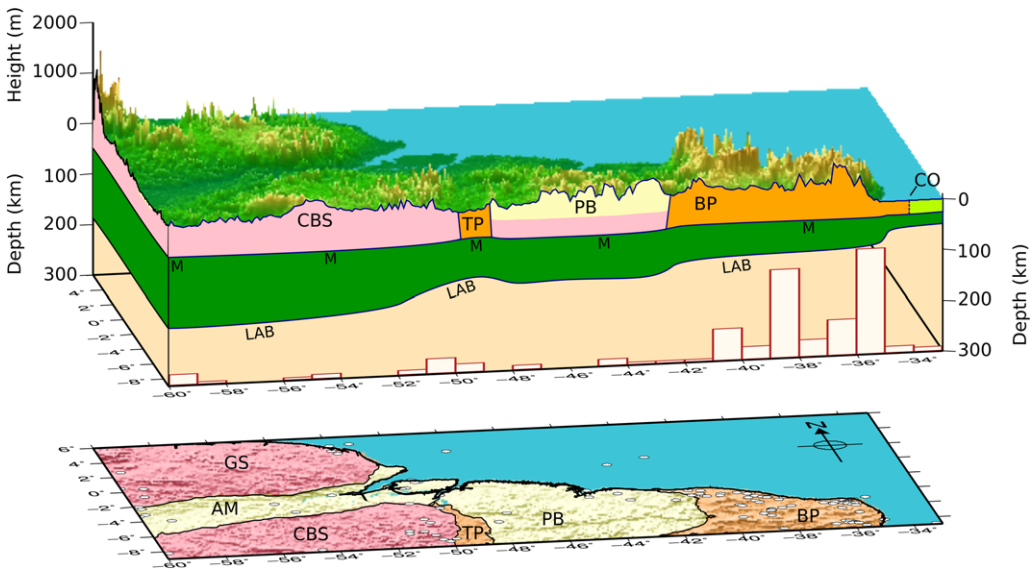
Fig. 12. Conceptual model showing lithospheric cross-section based on real data from northern Brazil. Histogram with white bars shows number of earthquakes per longitudinal degree from the considered area. Topography is exaggerated $100\times$. CO, continental–oceanic crustal limit; M, Moho discontinuity; LAB, lithosphere–asthenosphere boundary; GS, Guyana Shield; CBS, Central Brazil Shield; AM, Amazonian Basin; PB, Parnaíba Basin; BP, Borborema Province; TP, Tocantins Province.

occurrence of intraplate seismicity. This methodology is easily transferable to other areas and thus comparisons between different intraplate regions of the world could be analysed in future studies. A possible next step would be to perform a multivariate regression to quantify and model the relative influence of each of the geophysical parameters on the occurrence of seismicity. A preliminary attempt shows that the variables with greater influence are elastic thickness and heat flow, in agreement with the findings presented here.

Conclusion

Seismicity in mid-plate South America was analysed and described as a function of the distribution of several geophysical parameters characterizing lithospheric properties. We found that seismicity does not occur homogeneously and tends to concentrate in areas characterized by certain ranges of values for each of the geophysical variables considered. Higher than average seismicity rates were observed for regions with: a positive free air gravity anomaly (greater than -10 mGal); a lower elastic thickness (<30 km); a higher heat flow (>80 mW m^{-2}); a thinner crust (between 20 and 35 km); and a negative S-wave anomaly in the lithospheric lid (less than -1%). In contrast, lower than average seismicity was observed for areas with: a

high elastic thickness (>100 km); a low heat flow (<70 mW m^{-2}); and a high S-wave anomaly ($>5\%$, characteristic of cratonic roots).

Areas with rifted crust (i.e. passive margins) did not have more seismicity than non-rifted crust areas. On the other hand, Neoproterozoic fold belts were found to be significantly more seismic than Phanerozoic basins and cratonic areas. The occurrence of more seismicity in fold belts can be explained by their geophysical characteristics (more likely to have thinned lithosphere, thinned crust, higher heat flow, lower elastic thickness and larger gravity anomalies), in agreement with the preferred ranges of geophysical values for earthquakes. Cratonic areas, in contrast, present characteristics that inhibit the occurrence of seismicity, such as a low heat flow, deep lithospheric roots and high elastic thickness.

All this can be unified into the concept of earthquake-prone areas with a hotter, weakened lithosphere, delimited by strong lateral geophysical variations. In these areas, the bulk of the lithospheric stresses are concentrated at the brittle upper crust, eventually leading to a higher occurrence of intraplate earthquakes.

References

Agurto, H., Rietbrock, A., Ryder, I. & Miller, M. 2012. Seismic-afterslip characterization of the 2010 Mw 8.8 Maule, Chile, earthquake based on moment tensor inversion. *Geophysical Research Letters*, **39**.

Agurto-Detzel, H., Assumpção, M., Ciardelli, C., Albuquerque, D. F., Barros, L. V. & França, G. S. 2015. The 2012–2013 Montes Claros earthquake series in the São Francisco Craton, Brazil: new evidence for non-uniform intraplate stresses in mid-plate South America. *Geophysical Journal International*, **200**, 216–226, https://doi.org/10.1093/gji/ggu333

Amante, C. & Eakins, B. W. 2009. *ETOPO1 1 Arc-Minute Global Relief Model: Procedures, Data Sources and Analysis*. NOAA Technical Memorandum NESDIS NGDC-24, https://doi.org/10.7289/V5C8276M

Assumpção, M. 1983. A regional magnitude scale for Brazil. *Bulletin of the Seismological Society of America*, **73**, 237–246.

Assumpção, M. 1998. Seismicity and stresses in the Brazilian passive margin. *Bulletin of the Seismological Society of America*, **78**, 160–169.

Assumpção, M. & Sacek, V. 2013. Intra-plate seismicity and flexural stresses in central Brazil. *Geophysical Research Letters*, **40**, 487–491.

Assumpção, M., An, M., Bianchi, M., França, G. S., Rocha, M., Barbosa, J. R. & Berrocal, J. 2004. Seismic studies of the Brasília fold belt at the western border of the São Francisco Craton, Central Brazil, using receiver function, surface-wave dispersion and teleseismic tomography. *Tectonophysics*, **388**, 173–185.

Assumpção, M., Feng, M., Tassara, A. & Julià, J. 2013*a*. Models of crustal thickness for South America from seismic refraction, receiver functions and surface wave tomography. *Tectonophysics*, **609**, 82–96.

Assumpção, M., Bianchi, M. *et al.* 2013*b*. Crustal thickness map of Brazil: data compilation and main features. *Journal of South American Earth Sciences*, **43**, 74–85.

Assumpção, M., Ferreira, J. *et al.* 2014. Intraplate seismicity in Brazil. *In*: Talwani, P. (ed.) *Intraplate Earthquakes*. Cambridge University Press, Cambridge, 50–71.

Azevedo, P. A., Rocha, M. P., Soares, J. E. & Fuck, R. A. 2015. Thin lithosphere between the Amazon and São Francisco Cratons, in Central Brazil, revealed by seismic P-wave tomography. *Geophysical Journal International*, **201**, 61–69.

Barros, L. V., Assumpção, M., Quintero, R. & Caixeta, D. 2009. The intraplate Porto dos Gaúchos seismic zone in the Amazon craton – Brazil. *Tectonophysics*, **469**, 37–47.

Berrocal, J., Assumpção, M., Antezana, R., Dias Neto, C., Ortega, R., França, H. & Veloso, J. A. 1984. *Sismicidade do Brasil*. IAG/USP and Comissão Nacional de Energia Nuclear, Sao Paulo, Brazil.

Bianchi, M. B. 2008. *Variações da estrutura da crosta, litosfera e manto para a pla- taforma Sul Americana atraves de funçoes do receptor para ondas P e S*. PhD thesis. IAG, University of São Paulo.

Brito Neves, B. B. 2002. Main stages of the development of the sedimentary basins of South America and their relationship with the tectonics of supercontinents. *Gondwana Research*, **5**, 175–196.

Chimpliganond, C., Assumpção, M., Von Huelsen, M. & França, G. S. 2010. The intracratonic Caraíbas–Itacarambi earthquake of December 9, 2007 (4.9 mb), Minas Gerais State, Brazil. *Tectonophysics*, **480**, 48–56.

Cogné, N., Gallagher, K., Cobbold, P. R., Riccomini, C. & Gautheron, C. 2012. Post-breakup tectonics in southeast Brazil from thermochronological data and combined inverse-forward thermal history modeling. *Journal of Geophysical Research*, **117**, https://doi.org/10.1029/2012JB009340

Davies, J. H. 2013. Global map of solid Earth surface heat flow. *Geochemistry, Geophysics, Geosystems*, **14**, 4608–4622.

Durrheim, R. J. & Mooney, W. D. 1994. Evolution of the Precambrian lithosphere: seismological and geochemical constraints. *Journal of Geophysical Research*, **99**, 15 359–15 374.

Gardner, J. K. & Knopoff, L. 1974. Is the sequence of earthquakes in Southern California, with aftershocks removed, Poissonian? *Bulletin of the Seismological Society of America*, **64**, 1363–1367.

Hamza, V. M., Dias, F. J., Gomes, A. J. & Terceros, Z. G. D. 2005. Numerical and functional representations of regional heat flow in South America. *Physics of the Earth and Planetary Interiors*, **152**, 223–256.

Hauksson, E. 2011. Crustal geophysics and seismicity in southern California. *Geophysical Journal International*, **186**, 82–98.

Heidbach, O., Tingay, M., Barth, A., Reinecker, J., Kurfess, D. & Müller, B. 2010. Global crustal stress pattern based on the World Stress Map database release 2008. *Tectonophysics*, **482**, 3–15.

Hough, S. E. 2014. Intraplate seismic hazard: evidence for distributed strain and implications for seismic hazard. *In*: Talwani, P. (ed.) *Intraplate Earthquakes*. Cambridge University Press, Cambridge, 303–327.

Johnston, A. C. & Kanter, L. R. 1990. Earthquakes in stable continental crust. *Scientific American*, **262**, 68–75.

Johnston, A. C., Coppersmith, K. J., Kanter, L. R. & Cornell, C. A. 1994. The earthquakes of stable continental regions: assessment of large earthquake potential. *In*: Schneider, J. F. (ed.) *The earthquakes of stable continental regions. Volume 1: Assesment of large earthquake potential*. TR-102261, Vols **1–5**. Electric Power Research Institute, Palo Alto.

Liu, L. & Zoback, M. D. 1997. Lithospheric strength and intraplate seismicity in the New Madrid seismic zone. *Tectonics*, **16**, 585–595.

Mooney, W. D., Ritsema, J. & Hwang, Y. K. 2012. Crustal seismicity and the earthquake catalog maximum moment magnitude (M_{cmax}) in stable continental regions (SCRs): correlation with the seismic velocity of the lithosphere. *Earth and Planetary Science Letters*, **357**, 78–83.

Pérez-Gussinyé, M., Lowry, A. R. & Watts, A. B. 2007. Effective elastic thickness of South America and its implications for intracontinental deformation. *Geochemistry, Geophysics, Geosystems*, **8**, Q05009, https://doi.org/10.1029/2006GC001511

Pérez-Gussinyé, M., Metois, M., Fernández, M., Vergés, J., Fullea, J. & Lowry, A. R. 2009*a*. Effective elastic thickness of Africa and its relationship to other proxies for lithospheric structure and surface tectonics. *Earth and Planetary Science Letters*, **287**, 152–167, https://doi.org/10.1026/j.epsl.2009.08.004

Pérez-Gussinyé, M., Swain, C. J., Kirby, J. F. & Lowry, A. R. 2009*b*. Spatial variations of the effective elastic thickness, T_e, using multitaper spectral estimation and wavelet methods: examples from synthetic data and application to South America. *Geochemistry, Geophysics, Geosystems*, **10**, Q04005, https://doi.org/10.1029/2008GC002229

R Core Team 2014. *R: A Language and Environment for Statistical Computing*. R Foundation for Statistical Computing, Vienna, Austria, www.R-project.org/

Schulte, S. & Mooney, W. D. 2005. An updated global earthquake catalogue for stable continental regions: reassessing the correlation with ancient rifts. *Geophysical Journal International*, **161**, 707–721.

Stein, S., Cloetingh, S., Sleep, N. & Wortel, R. 1989. Passive margin earthquakes, stresses, and rheology. *In*: Gregerson, S. & Basham, P. (eds) *Earthquakes at North-Atlantic Passive Margins: Neotectonics and Postglacial Rebound*. Kluwer, Dordrecht, 231–260.

Sykes, L. R. 1978. Intraplate seismicity, reactivation of preexisting zones of weakness, alkaline magmatism, and other tectonism postdating continental fragmentation. *Reviews of Geophysics and Space Physics*, **16**, 621–688.

Talwani, P. 1999. Fault geometry and earthquakes in continental interiors. *Tectonophysics*, **305**, 371–379.

Talwani, P. 2014. Unified model for intraplate earthquakes. *In*: Talwani, P. (ed.) *Intraplate Earthquakes*. Cambridge University Press, Cambridge, 275–327.

Uhrhammer, R. 1986. Characteristics of northern and central California seismicity. *Earthquake Notes*, **57**, 21.

Wessel, P. & Smith, W. 1998. New, improved version of generic mapping tools released. *Eos, Transactions of the American Geophysical Union*, **79**, 579.

Zoback, M. L. 1992. First- and second-order patterns of stress in the lithosphere: the world stress map project. *Journal of Geophysical Research*, **97B**, 11 703–11 728.

Zoback, M. L. & Richardson, R. M. 1996. Stress perturbation associated with the Amazonas and other ancient continental rifts. *Journal of Geophysical Research*, **101**, 5459–5475.